Single-Element Switched-Beam Antenna Utilizing a Radial-Basis Function Network

Pichaya Chaipanya and Sunisa Kunarak
Department of Electrical Engineering, Srinakharinwirot University, Nakhon Nayok 26120, Thailand
Email: pichayac@g.swu.ac.th; sunisaku@g.swu.ac.th

Abstract**—**This article presents beam switching at a mobile terminal using only a single-element antenna. There are eight different directions which are controlled by shorted and open circuits at the edge of a radiating patch. Shorted and open circuits were considered for use in a radial-basis function network to operate a suitable beam at a mobile terminal. The mean square error of beam selection was 5.31×10^{-33}, which can confirm that the proposed radial-basis function network provides accuracy in selecting the main beam direction toward the cell site. Moreover, the article reveals that the performance in terms of SIR and channel capacity confirms a performance improvement when the proposed concept is utilized.

Index Terms**—**Switched beamforming, shorted circuit, neural network, radial basis function, mobile terminal

I. Introduction

Smart Antenna Systems is one technique that can manage the demand of increasing users in wireless communications. The switched-beam antenna is one category of smart antenna [1], [2] that is capable of improving wireless systems. Switched-beam antennas are constituted of an antenna array, a simple beam-forming network and a beam selector. There is an array with multiple fixed beams in different directions, which are produced in the beam-forming network. Then, the correct beam is searched for by the beam selector. However, to apply the switched beam at mobile terminals, the small size and low complexity of switched-beam antennas are focused on. Several researchers have proposed a small-structured and low-complexity switched-beam antenna, such as in the work presented in [3]: a low-profile tilted-beam single-arm spiral antenna on a high-impedance surface for beam-steering applications. The antenna has four feeding points which the radiation patterns can be steered towards by changing the feeding points. This should be not practical as the feeding network is relatively complicated. The work proposed in [4] described a performance evaluation of a low-cost switched-beam antenna for WLAN users. This work proposed a single octagonal-patch antenna which is capable of beam switching in eight directions by shorted-circuit terminations at the edges of the patch. The average gain in all directions was 3.48 dB. Moreover, the work presented in [5] proposed a low-profile switched beam utilizing a ring-parasitic antenna. There are eight different directions which the beam direction can be changed towards by shorted circuits on different small circular elements of the parasitic ring. The average gain of the antenna when eight cases of shorted circuit are applied is 4.758 dBi. However, the parasitic ring is a rather complex structure.

In addition, the artificial neural network is one system that has been applied to make decisions with regard to switching the beam selection in the antenna. The works presented in [6], [7] have disclosed a neural-network-based switched-beam smart antenna and implementation of the switched-beam smart antenna using an artificial neural network. The 4×4 Butler matrix is used in these works to switch the beam pattern in four directions. A feed-forward back-propagation neural network is used to control the switched-beam smart antenna depending on the user's equipment position. After training the built network, accuracy of beam selection is obtained. However, these works proposed beam switching to cover the mobile position from the base station. However, any failure in smart antenna systems installed at a base station may cause undesirable damage for all users. Moreover, learning can be slow when there is a lot of data input using a feed-forward back-propagation neural network. Therefore, this article proposes a switched-beam antenna using a single element in which the beam is selected using a radial-basis function network at the mobile terminal. This concept allows the network to be able to handle the increase in input data. Moreover, the proposed concept maintains accuracy in beam switching when the position of the user is changed.

The rest of this article is structured as follows. After a brief introduction, the proposed antenna design is discussed in Section II. Next, the radial-basis function network which cooperates with the single-element switched-beam antenna is discussed in Section III. The performance in terms of SIR and channel capacity are revealed in this section. Finally, Section IV concludes the article.

II. Single-Element Switched-Beam Antenna

To reduce the size of the switched-beam antenna, the single-element switched-beam antenna has been focused on. The circular patch has been adopted for this article.

Manuscript received September, 2017; revised November 15, 2017.
This work was supported by Faculty of Engineering, Srinakharinwirot University under Grant No. 375/2559.
Corresponding author email: pichayac@g.swu.ac.th
doi:10.12720/jcm.12.11.630-635

The proposed antenna has been designed on FR4 with a dielectric constant of 4.3 and substrate thickness of 2.00 mm. The antenna consists of a circular radiating patch on the center with a radius of *a*, which can be obtained by [8],

$$a = \frac{F}{\left\{1 + \frac{2h}{\pi \varepsilon_r F}\left[\ln\left(\frac{\pi F}{2h}\right) + 1.7726\right]\right\}^{1/2}} \tag{1}$$

where

$$F = \frac{8.791 \times 10^9}{f_r \sqrt{\varepsilon_r}} \tag{2}$$

where f_r stands for resonant frequency, ε_r is dielectric constant, and the height of the substrate is h in cm. However, the obtained radius from (1) is 17.046 mm, which is a small size for designing the positions of the shorted and open circuits. Therefore, the size of the circular patch has been increased to *2a*, 34.093 mm, which is a size big enough for the design of the shorted and open positions. Next, the SMA feed probe was attached from one side through to the other side at the center of the patch, which is symmetrically positioned along the E-plane. However, the radiation pattern is affected by the position of the feed probe, size of substrate and ground plane. This is due to the fact that the feed position is fixed to a symmetrical position. Therefore, the sizes of the circular patch, substrate and ground plane have been adjusted to the switchable beam. Thus, the size of the patch is 32 mm, while the ground plane and substrate are the same size, namely 98×98 mm^2.

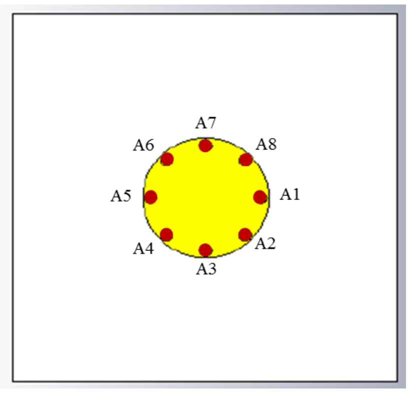

Fig. 1. Configuration and shored positions of switched-beam antenna

Next, beam switching was controlled by the shorted and open circuits at the edge of the circular patch. There are eight positions of short and open circuit, A1 to A8, as shown in Fig. 1. The main beam direction is changed when the positions of short and open circuits are alternated. Radiation patterns of the antenna, obtained from CST Microwave Studio, are shown in Fig. 2 to Fig. 5. In Fig. 2, the main beam directions are 0° and 180° when A1 and A5 are open while others are shorted, so called beam 1 and beam 5, respectively. The main beam directions are 45° and 225° when A2 and A6 are open while others are shorted, so called beam 2 and beam 6, as shown in Fig. 3. In Fig. 4, the main beam directions are 90° and 270° when A3 and A7 are open, so called beam 3 and beam 7, respectively. Also, beam 4 and beam 8, where the main beam directions are 135° and 315° when A4 and A8 are open, are shown in Fig. 5. The average gain of the eight directions was 5.495 dBi. This result indicates that a beam can be switched using only a single element. Moreover, the proposed antenna is considerably attractive as it is small in size, easy to manufacture and exhibits high gain.

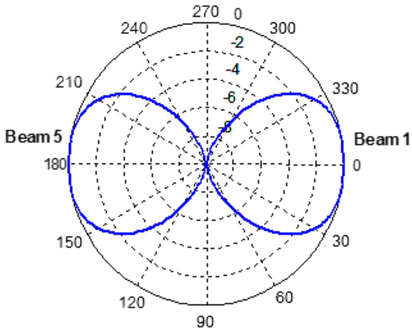

Fig. 2. Radiation patterns when A1 and A5 are open.

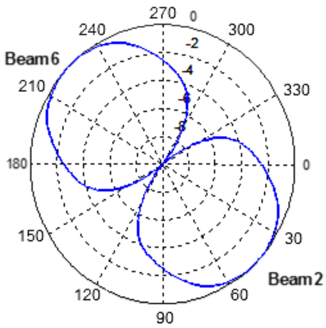

Fig. 3. Radiation patterns when A2 and A6 are open.

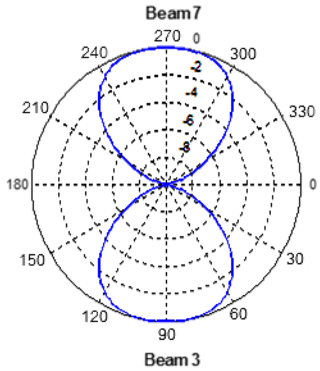

Fig. 4. Radiation patterns when A3 and A7 are open.

Next, the eight main beam directions of the proposed antenna cooperated with the radial basis function network. The direction between the mobile user and the cell site was calculated. Moreover, the impacts of the interference signals that appear on two adjacent beams were considered. After that, the network was trained to select the positions of shorted and open circuits to produce a suitable beam that provides high performance.

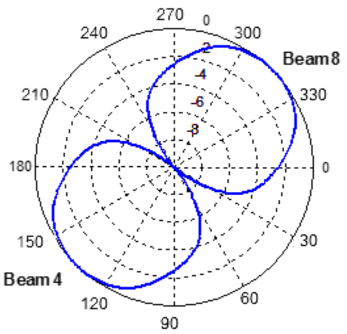

Fig. 5. Radiation patterns when A4 and A8 are open.

III. Radial Basis Function Network with Switched-Beam Formation

The radial-basis function was used to control the position of shorted and open circuits to switch the beam pattern depending on the direction between mobile user and cell site. The beam of a mobile terminal that was directed towards the cell site was selected, as shown in Fig. 6. However, in cases where the position of the cell site was located between two adjacent beams, as shown in Fig. 7, the impact of interference signals that appear on two adjacent beams was compared. Then, the most suitable beam was selected.

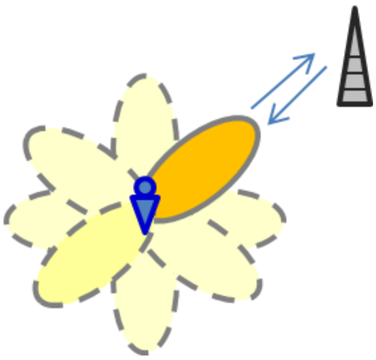

Fig. 6. Beam 8, which can cover the cell site, is selected.

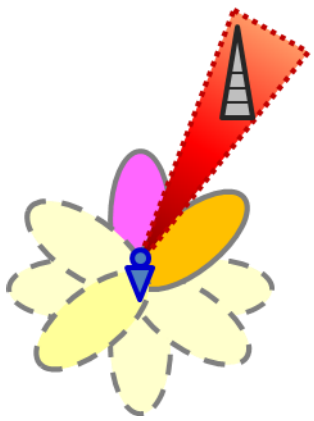

Fig. 7. Beam 1 or beam 8 can be selected.

Radial basis function is constituted of three layers: input layer, hidden layer and output layer. Each input node in the input layer is fully connected to the hidden node in the hidden layer. There is a Gaussian activation function in the hidden layer which is expressed by

$$G(\mathbf{x},\mathbf{x}_i)=\exp\left(-\frac{1}{2\sigma_i^2}\|\mathbf{x}-\mathbf{x}_i\|^2\right) \tag{3}$$

where $\mathbf{x}$ and $\mathbf{x_i}$ are input vectors and the center of the function, respectively. σ is standard deviation (width/ span). Next, each output of the hidden node is connected to the output layer after the weight value has been calculated, as shown in Fig. 8. The weight values are adjusted until the output has good correlation with the target, in which the performance function is Mean Square Error (MSE) that can be obtained by

$$MSE=\frac{1}{N}\sum_{i=1}^{N}\left(\text{Target}_i-\text{Output}_i\right)^2 \tag{4}$$

where N is the number between the network outputs and the desired outputs. Target and Output represent the desired outputs and the network outputs, respectively.

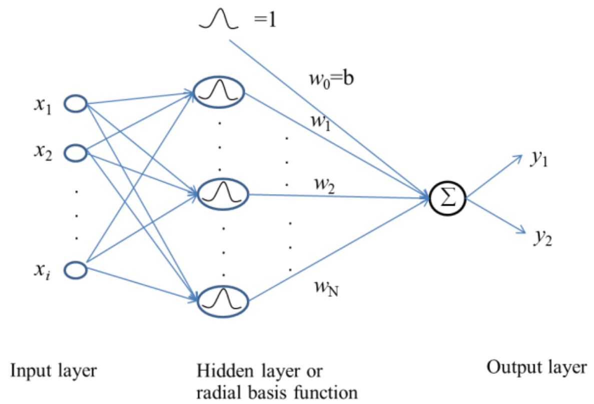

Fig. 8. Configuration of radial-basis function networks.

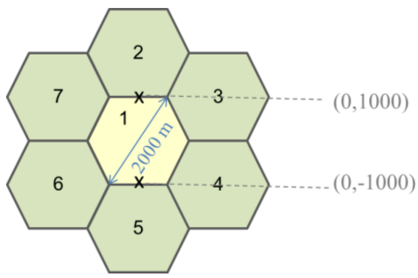

Fig. 9. The structure of a 1-tire 7 cells.

TABLE I: THE TRAINING PARAMETERS OF RADIAL-BASIS FUNCTION

Parameters	Values
number of input neurals	4
number of hidden layer	1
number of neural in the hidden layer	3
number of output neurals	8
No. of epochs	3
training time (s)	0.04

In this article, the training parameters of the radial-basis function are listed in Table I. The network was trained by using the positions of the mobile users and the cell site. After that, comparison of the interference signals between two adjacent beams was considered. The environment with a-tier 7 cells is assumed in this article, in which the radius of a cell is 1000 m as shown in Fig. 9.

TABLE II: THE CONDITION OF BEAM SWITCHING

Beam	positions of open circuit	Main beam directions	Direction between user and cell site	Direction of adjacent beams
1	A1, A5	0 °	0 °– 15 °, 345 °- 360 °	
2	A2, A6	45 °	30 °– 60 °	15 °- 30 °
3	A3, A7	90 °	75 °- 105 °	60 °– 65 °
4	A4, A8	135 °	120 °– 150 °	105 °– 120 °
5	A1, A5	180 °	165 °– 195 °	150 °- 165 °
6	A2, A6	225 °	210 °– 240 °	195 °– 210 °
7	A3, A7	270 °	255 °– 285 °	240 °– 255 °
8	A4, A8	315 °	300 °– 330 °	285 °– 300 °
1	A1, A5			330 °– 345 °

TABLE III: THE OBTAINED RESULTS FROM RADIAL-BASIS FUNCTION WITH BEAM SWITCHING

X-Axis, Y-Axis	No. of Cell	Direction	Target		Output	
			positions of open circuit	beam	positions of open circuit	beam
-2295.0, 844.3	7	152.17	A4, A8/ A1, A5	4/ 5	A1, A5	5
922.9, 1494.8	2	28.69	A1, A5/ A2, A6	1/ 2	A2, A6	2
1440.2, -1591.0	4	133.44	A4, A8	4	A4, A8	4
2823.6, 2201.6	3	304.42	A4, A8	8	A4, A8	8
-801.4, -784.8	1	135.59	A4, A8	4	A4, A8	4
587.6, 1736.2	2	24.17	A1, A5/ A2, A6	1/ 2	A2, A6	2
-1763.8, -2480.0	6	80.93	A3, A7	3	A3, A7	3
-1766.0, -670.4	6	305.37	A4, A8	8	A4, A8	8
-1626.3, 851.6	7	21.65	A1, A5/ A2, A6	1/ 2	A2, A6	2
-2088.9, 1691.6	7	262.67	A3, A7	7	A3, A7	7
-1235.6, -1575.8	6	36.98	A2, A6	2	A2, A6	2
-2451.0, -568.1	6	223.75	A2, A6	6	A2, A6	6
-2326.3, 1706.6	7	245.21	A2, A6/ A3, A7	6/ 7	A2, A6	6
621.2, 2786.5	2	308.30	A4, A8	8	A4, A8	8
1168.5, 1548.6	3	213.41	A2, A6	6	A2, A6	6
933.0, -2341.5	5	20.10	A1, A5/ A2, A6	1/ 2	A2, A6	2
-1875.2, -1402.9	6	72.79	A3, A7	3	A3, A7	3
-74.4, 1613.7	2	100.89	A3, A7	3	A3, A7	3
-1362.4, -2776.6	6	70.25	A2, A6/ A3, A7	2/ 3	A3, A7	3
-422.6, -289.6	1	145.58	A4, A8	4	A4, A8	4

The direction between the mobile user and the cell site was calculated. Next, positions of shorted and open circuits to operate a suitable beam at the mobile terminal were selected by radial basis function; the conditions of beam switching are shown in Table II. In addition, the impact of interference signals that appear in each beam when the cell site is located between two adjacent beams was considered. A beam where interference has a low impact was selected. Some of the obtained results of shorted and open circuits are shown in Table III when the positions of the user and interference signals are random. As we can see, it takes hardly any time to train the network due to the low-complexity switching condition. Moreover, the MSE is 5.31×10^{-33} at only 3 epochs, as shown in Fig. 10, which can confirm that the proposed radial-basis function networks applied to a switched-beam Smart Antenna System exhibit a high level of accuracy and a low level of complexity.

Next, the performance in term of SIR is revealed when a distance between adjacent cells of 1000 to 3000 meters is assumed. The received SIR at i^{th} user can be obtained by [9], [10]

$$SIR_i = \frac{P_i g_i \left(10^{\frac{PL_i}{10}}\right)}{\sum_j P_j g_{i,j} \left(10^{\frac{PL_j}{10}}\right)} \tag{5}$$

where the P_i and P_j are the transmitted power servings at the i^{th} cell and interfering j^{th} cell, respectively. The g_i is the gain of the antenna when the i^{th} user received the signal from the cell site. In addition, $g_{i,j}$ is the gain observed between the i^{th} user and the j^{th} cell site. The PL_i and PL_j are propagation path losses from the i^{th} cell site and the j^{th} cell site to the i^{th} user, respectively. The path loss effect in a wireless channel between users and a cell site can be expressed by

$$PL = 20\log_{10}\left(\frac{4\pi d}{\lambda}\right) \tag{6}$$

where d is the distance between the user and the cell site.

The performance in terms of SIR and channel capacity when the proposed concept was applied was compared with the conventional concept, in which an omni-directional antenna is used, as shown in Fig. 11 and Fig. 12. It is apparent that the SIR and channel capacity can be clearly enhanced when utilizing the proposed concept. Moreover, in cases where the cell site was located between two adjacent beams, the SIR and channel capacity when using the proposed concept were still higher than when using the conventional concept. This is because the interference signals were reduced.

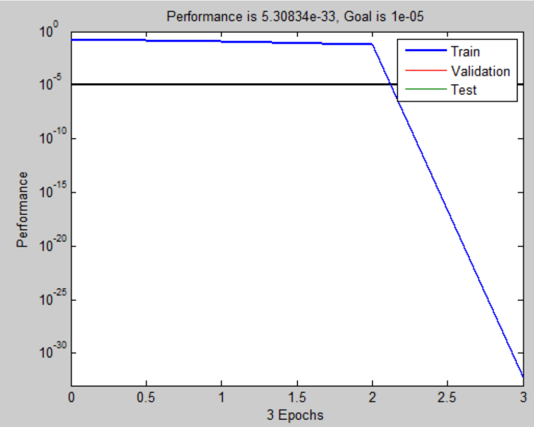

Fig. 10. The performance function in term of MSE.

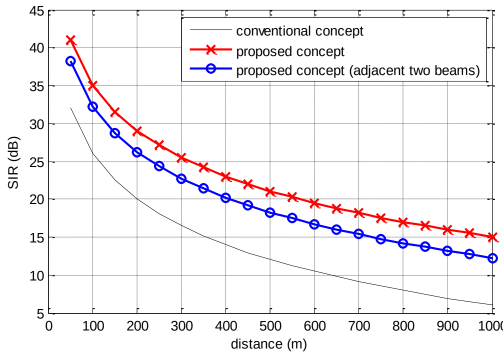

Fig. 11. SIR vs. distance between cell site and users.

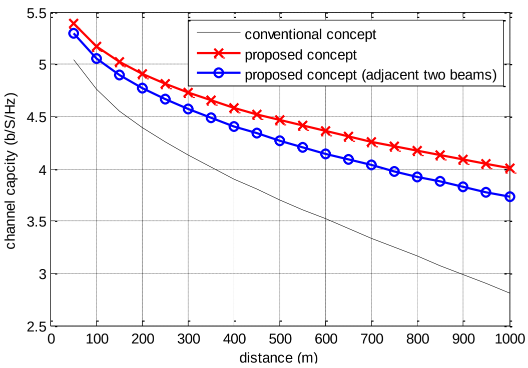

Fig. 12. Channel capacity when distance between user and cell site is varied.

IV. Conclusions

This article proposes a circular-patch switched-beam antenna using a single element. There are eight different main beam directions: 0°, 45°, 90°, 135°, 180°, 225°, 270° and 315°. They are controlled by shorted and open circuits at the edge of the radiating circular path. The proposed antenna cooperates with a radial-basis function network. The positions of shorted and open circuits are selected to provide a suitable beam based on the position of the user with regard to the cell site. Moreover, in cases where the position of the cell site is located between two adjacent beams, interference signals that appear on each beam are considered and the most suitable beam is selected. The results confirm the accuracy of the proposed concept, which showed a performance function in terms of MSE equal to 5.31×10^{-33}. In addition, the performance in terms of SIR and channel capacity was revealed. The obtained results indicate that the performance of systems can improve when the proposed concept is employed, when compared to the ones utilizing an omni-directional antenna. Further work includes implementation of antenna and radial-basis function network for testing the performance in real environment.

Acknowledgment

Financial support from the Faculty of Engineering, Srinakharinwirot University, through the research grant No. 375/2559 is acknowledged.

References

[1] B. G. Frank, *Smart Antenna for Wireless Communications with MATLAB*, 1st ed., McGraw-Hill, 2005, ch.8.

[2] J. C. Liberti and T. S. Rappaport, *Smart Antennas fot Wireless Communications IS-95 and Third Generation CDMA Applications*, 1st ed., Prentice Hall PTR, 1999, ch.3.

[3] A. Mehta, A. Sanada, D. Mirshekar-Syhakal, and H. Nakano, "A low profile tilted beam single arm spiral antenna on a high impedance surface for beam steering applications," in *Proc. International Workshop on Antenna Technology: Small and Smart Antennas Metamaterials and Applications*, Cambridge, UK., 2007, pp. 408-411.

[4] M. Uthansakul, P. Chaipanya, and P. Uthansakul, "Performance evaluation of a low-cost switched-beam antenna for WLAN users," *Microwave and Optical Technology Letters*, vol. 52, no. 9, pp. 2069-2074, September 2010.

[5] P. Chaipanya, "Low profile switched beam utilizing a ring-parasitic antenna," in *Proc. International Symposium Antennas and Propagation*, Hobart, TAS, Australia 2015, pp. 1-4.

[6] S. I. Orakwue, R. Ngah, T. A. Rahman, and S. Z. Mohd Hashim, "Neural network based switch beam smart antenna," in *Proc. IEEE Asia Pacific Conference on Wireless and Mobile*, Bali, Indonesia 2014, pp. 292-296.

[7] S. I. Orakwue, R. Ngah, T. A. Rahman, S. Z. Mohd, and H. H. M. R. Al-Khafaji, "Implementation of switched beam smart antenna using artificial neural network,"

Wireless Personal Communications, vol. 83, no. 1, pp. 87-98, July 2015.

[8] C. A. Balanis, *Antenna Theory Analysis and Design*, 3rd ed., New Jersey: J. Wiley & Sons, 2005, ch.14.

[9] A. Goldsmith, *Wireless Communications*, New York: Cambridge University Press, 2007. ch.4.

[10] F. Khan, *LTE for 4G Mobile Broadband Air Interface Technologies and Performance*, New York: Cambridge University Press, 2009. ch.16.

Pichaya Chaipanya was born in Thailand on November, 1985. She received the B.S., M.S. and Ph.D. degrees in telecommunication engineering from Suranaree University of Technology (SUT), Nakhon Ratchasima, Thailand in 2007, 2009 and 2014, respectively. Now she is lecturer in Department of Electrical Engineering, Srinakharinwirot University (SWU), Thailand. Her research interest is focused on smart antenna systems and wireless communications.

Sunisa Kunarak was born in Chonburi, Thailand, on December, 1980. She received the B.S. degree in electrical engineering (electronics and telecommunication) and M.S. degree in electrical engineering from King Mongkut's University of Technology Thonburi, Thailand in 2002 and 2004, respectively. She is currently a lecturer of digital logic and mobile wireless communications at Srinakharinwirot University in Thailand where she heads the digital laboratory. Her current research interests include mobile communications and broadband wireless networks.